Available online at www.sciencedirect.com
SCIENCE DIRECT
Polymer 47 (2006) 858–870
polymer
www.elsevier.com/locate/polymer

Gas transport through nano and micro composites of natural rubber (NR) and their blends with carboxylated styrene butadiene rubber (XSBR) latex membranes

Ranimol Stephen [a], C. Ranganathaiah [b], Siby Varghese [c], Kuruvilla Joseph [d], Sabu Thomas [a,*]

[a] School of Chemical Sciences, Mahatma Gandhi University, Kottayam 686 560, Kerala, India
[b] Department of Studies in Physics, University of Mysore, Manasagangotri, Mysore 570 006, India
[c] Rubber Research Institute of India, Kottayam, Kerala, India
[d] Post Graduate Department of Chemistry, St. Berchmans College, Changanacherry, Kerala, India

Received 19 April 2005; received in revised form 25 November 2005; accepted 8 December 2005

Abstract

The gas permeability coefficient of nano and micro composites of natural rubber, carboxylated styrene butadiene rubber and 70:30 natural rubber/carboxylated styrene butadiene rubber blend membranes has been investigated with special reference to type of filler, gases, filler loading and pressure. The layered silicates such as sodium bentonite and sodium fluorohectorite were the nanofillers used and the conventional micro fillers were clay and silica. Latex nanocomposites were characterized by X-ray diffraction technique. The dispersion of layered silicates in the polymer matrix was analysed using transmission electron microscopy. The fluorohectorite silicate showed excellent dispersion in natural rubber matrix. The effect of free volume on the gas barrier properties was investigated by positron annihilation lifetime spectroscopy. It was observed that due to the platelet like morphology and high aspect ratio of layered silicates, the gas barrier properties of nano filled latex membranes were very high. The crosslink density values and extent of reinforcement were estimated in order to correlate with the gas barrier properties. The oxygen/nitrogen selectivity of these membranes were investigated. The diffusion of gas molecules through the polymer was determined by time-lag method and diffusion selectivity of the membranes was computed.

Keywords: Latex membrane; Nano and micro fillers; Permeability

1. Introduction

Membranes of polymers have played an important role in many applications such as gas and liquid separations and barriers for packing [1–5]. The transport of gases through a membrane depends on various factors like permeant size and shape, permeant phase, polymer molecular weight, functional groups, density and polymer structure, crosslinking, crystallinity, orientation, etc. [6]. The wide application of membranes for gas separation has attracted many polymer technologists to synthesis new polymeric membranes with good permeability and selectivity [7–9]. Paul and co-workers [10–14] have investigated the relationship between gas transport and polymer structure. The introduction of functional groups in the polymer chain can alter the permeability and selectivity due to the variation in the existing free volume within the polymer [15,16]. The selective transport of gases through polymeric membranes has been reviewed by Aminabhavi and co-workers [17]. van Amerogen [18,19] extensively studied the permeability of various gases through different elastomers. Thomas and co-workers [20,21] investigated the gas transport properties of various rubber blends. They concluded that permeation is a process in which gas molecules dissolve in the elastomer on one side of a membrane, diffuse through it to the other side and then evaporate. The rate of diffusion in a given polymer is found to be related chiefly to the size of the gas molecule. It is observed that the presence of polar groups or methyl groups in the polymer molecule reduces the permeability of a given gas. In the case of permeant gases such as nitrogen, oxygen, and hydrogen, the permeability depends on the nature of gas, the membrane material, temperature and pressure.

* Corresponding author. Tel.: +91 481 2730003/91 481 2597914; fax: +91 481 2731001/91 481 2731009.
E-mail addresses: sabut@sancharnet.in (S. Thomas), sabut552001@yahoo.com (S. Thomas).

0032-3861/$ - see front matter © 2005 Elsevier Ltd. All rights reserved.
doi:10.1016/j.polymer.2005.12.020

The main goal for the addition of fillers to rubbers is to improve the properties and to cheapen the compound. The reinforcing ability of fillers depends on the particle size, structure, surface characteristics, filler origin and degree of dispersion [22–25]. Recently, polymer layered silicates nanocomposites have attracted many polymer technologists due to the dramatic improvement in mechanical and electrical properties, heat resistance, radiation resistance and gas barrier properties of polymers [26–31]. Polymer–clay nanocomposites based on organic polymers and inorganic clay minerals consisting of silicate layers is the most promising nanocomposite system [32–34]. Nowadays, there are lots of studies on the properties of polymer nanocomposites [36,37].

The platelet structure of layered silicates has the ability to improve the barrier properties of polymer materials according to a tortuous path model in which a small amount of platelet particles significantly reduce the permeability of gases through the nanocomposite. In the exfoliated system the individual clay platelets will have the highest aspect ratio and as a result the barrier properties get improved. Matayabas and co-workers [34] studied the enhancement in gas barrier properties of polyethylene terephthalate upon the addition of nano clay.

The aim of the present study is to investigate the gas transport properties of 70:30 natural rubber/carboxylated styrene butadiene rubber blend and individual polymers containing layered silicates and conventional micro fillers. Recently, Varghese et al. [35–37] studied the properties of natural rubber and synthetic rubber lattices reinforced with layered silicates. However, to our knowledge till date no systematic studies have been conducted on the gas barrier properties of latex membranes containing layered silicates. Recently, the authors have investigated the gas transport, mechanical and dynamic mechanical properties of NR/XSBR latex blends [38,39].

2. Experimental

2.1. Materials used

Natural rubber latex with 60% dry rubber content was procured from Gaico Rubbers Ltd, Kuravilangadu. The synthetic latex containing 47% dry rubber content was obtained from Apar Industries Ltd, Mumbai. The micro fillers such as clay and precipitated silica used were of commercial grade. The particle size of precipitated silica was 25 nm. The naturally occuring layered silicate purified sodium bentonite clay was obtained from Sud Chemie, Germany. The synthetic clay sodium fluorohectorite was collected from Coop Chemicals, Japan. The cation exchange capacity of sodium bentonite and sodium fluorohectorite is 80 and 100 mequiv./100 g and the interlayer distance is 1.24 and 0.94 nm, respectively.

2.2. Preparation of samples

Prevulcanization of latices was carried out by heating the compounded latex using water bath at 70 °C for 2 h. A 10% aqueous dispersions of layered silicates were added to the latex in varying amount with slow stirring. It was then filtered through a 250 μm mesh size sieve for removing the impurities. The weight percentage of layered silicates and micro fillers used were 2.5, 5 and 7.5% for 100 rubbers. In the sample code N stands for NR, the subscripts 100, 70 and 0 indicate weight percentage of NR, sP denotes sulphur prevulcanization, E, F, C and Si represents sodium bentonite, sodium fluorohectorite, clay and silica, respectively.

2.3. X-ray diffraction analysis of layered silicates

X-ray diffraction patterns were taken by using Ni-filtered Cu K_α radiation ($\lambda = 0.154$ nm) by X'pert diffractometer, Philips at 40 keV and 30 mA. The samples were scanned in step mode by 1.5°/min scan rate in the range of $2\theta < 12°$.

2.4. Transmission electron microscopic analysis

Transmission electron micrographs of layered silicates reinforced latex nanocomposites were taken in a LEO 912 Omega transmission electron microscope with an acceleration voltage of 120 keV. The specimens were prepared using an Ultracut E cryomicrotome. Thin sections of about 100 nm were cut with a diamond knife at −120 °C.

2.5. Positron annihilation lifetime spectroscopic analysis

Positron annihilation lifetime spectra were recorded for nano and micro filled latex samples using Positron Annihilation Lifetime Spectrometer (PALS). The Positron Lifetime Spectrometer consists of a fast–fast coincidence system with BaF_2 scintillators coupled to photo multiplier tubes type XP2020/Q with quartz window as detectors. The detectors were shaped to conical to achieve better time resolution. A17mCi ^{22}Na positron source, deposited on a pure Kapton foil of 0.0127 mm thickness was placed between the two identical pieces of the sample under investigation. This sample-source sandwich was positioned between the two detectors of PALS to acquire lifetime spectrum. The spectrometer measures 180 ps as the resolution function with ^{60}Co source.

However, for better count rate, the spectrometer was operated at 220 ps time resolution [40]. All lifetime measurements were performed at room temperature and two to three positron lifetime spectra with more than a million counts under each spectrum were recorded. In PALS analysis only two measured parameters namely *o*-Ps life time (τ_3) and *o*-Ps intensity I_3. The *o*-Ps lifetime τ_3 measures the size of the free volume holes (V_f) and I_3 is a relative measure of the number of free volume sites in the polymer matrix.

The free volume cavity radius (R) is related to the *o*-Ps pick-off lifetime (τ_3) by a simple relation. The underlying assumption in the formulation of this relation is that *o*-Ps atom in a free volume cell can be approximated to a particle in a potential well of radius R_0. The potential is infinite if $r > R_0$ and constant for $r \leq R_0$. Further, it is assumed that there is an electron layer in the region $R < r < R_0$, with $R_0 = R + \delta R$ where δR represents the thickness of the electron layer or the

probability of overlap of the Ps wave function and electron wave function. The expression connecting the free volume radius R (in nm) and the *o*-Ps pick-off lifetime τ_3 (in ns) according to Nakanishi et al. [41] is

$$\left(\frac{1}{\tau_3}\right) = 2\left[1-\left(\frac{R}{R_0}\right)+\left(\frac{1}{2\pi}\right)\sin\left(\frac{2\pi R}{R_0}\right)\right] \quad (1)$$

Here, the value of $\delta R = 0.1656$ nm was determined by fitting experimental τ_3 values to data from molecular materials with well-known hole sizes like zeolites [42]. Using this value of R, the free volume size (V_f) is calculated as $V_f = (4/3)\pi R^3$. Then the relative fractional free volume is evaluated as the product of free volume (V_f) and *o*-Ps intensity, I_3 (%).

2.6. Permeability measurements

The measurements were done using ATS FAAR gas permeability tester in manometric method in accordance with the ASTM standard D1434. The permeability of O_2 and N_2 gas through NR, XSBR and NR/XSBR latex blends was tested at various pressures.

2.7. Crosslink density measurements

Crosslink density values of the samples were determined by equilibrium swelling method-using toluene. For the experiment circular samples were punched from the sheet and the weighed samples were kept in toluene until equilibrium reached, then the weights were taken for the calculation.

3. Results

3.1. X-ray diffraction analysis

X-ray diffraction technique is the most widely used for the characterization of structure of layered silicate and polymer nanocomposites, and provides globally averaged information, potentially over six or more orders of magnitude. The change in interlayer spacing, i.e. the *d*-spacing of the latex nanocomposites is observed from the peak position in the XRD graphs in accordance with Bragg equation,

$$n\lambda = 2d\sin\theta \quad (2)$$

where n is an integer, λ is the wavelength, d is the interlayer spacing and θ is the angle of diffraction. The X-ray diffraction pattern of the layered silicates and latex nanocomposites are given in Fig. 1. The interlayer spacing of latex nanocomposites is found to increase with the incorporation of clay. In the case of exfoliated structure, layer separation associated with the delamination of the silicate structure in the polymer matrix leading to the disappearance of X-ray scattering. It may be due to either the presence of an extremely large regular ordered spacing between the layers, or the nanocomposite no longer has an ordered layer structure.

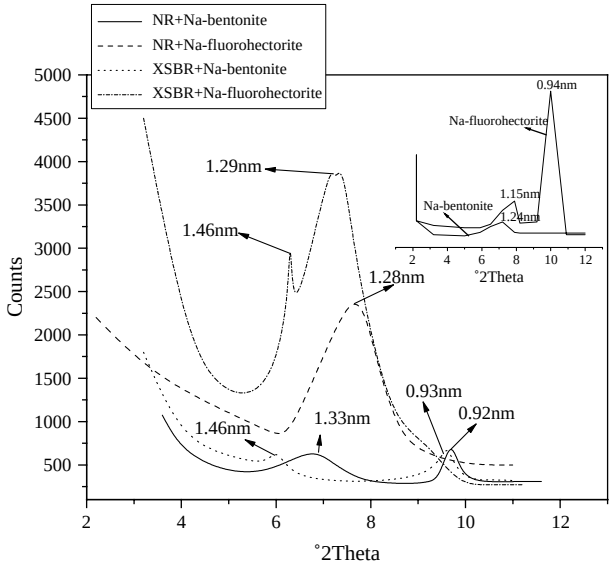

Fig. 1. X-ray diffraction patterns of layered silicates and latex nanocomposites.

3.2. Transmission electron microscopic analysis

Transmission electron microscopy is the most important method for the analysis of dispersion of layered silicates in polymer nanocomposites. The dispersion of layered silicates in NR latex has been investigated by TEM. Fig. 2(a)–(c) shows the transmission electron micrographs of commercial clay, sodium bentonite and sodium fluorohectorite respectively. From Fig. 2(a) we can see that the commercial clay exists as aggregates and the dispersion is not uniform. Sodium bentonite filled latex nanocomposites show some level of intercalation and aggregation of silicates (Fig. 2(b)) while exfoliated structure is predominant in the case of sodium fluorohectorite reinforced latex nanocomposites (Fig. 2(c)).

3.3. Positron annihilation lifetime spectroscopic (PALS) analysis

An understanding of the free volume property of polymers is crucial for determining the permeability and ionic conductivity of polymers. Nowadays, positron annihilation spectroscopic analysis is carried out for the experimental quantification of free volume [43,44]. This method helps one to estimate the hole size at a nanoscale and its fraction directly. It has been found that the estimated hole size and fraction significantly relate to the free volume property of polymer materials [43,44]. Ito and co-workers [45] examined the relationship between the oxygen permeability and the free volume for ethylene–vinyl alcohol copolymer as the ethylene content varies, which significantly followed the free volume theory. The results obtained for them suggest that the molecular mechanism of gas permeation could be considered on the basis of the local motion of the polymer segments and the free volume size. Nagel et al. [46] correlated the free volume and transport properties of highly selective polymer membranes.

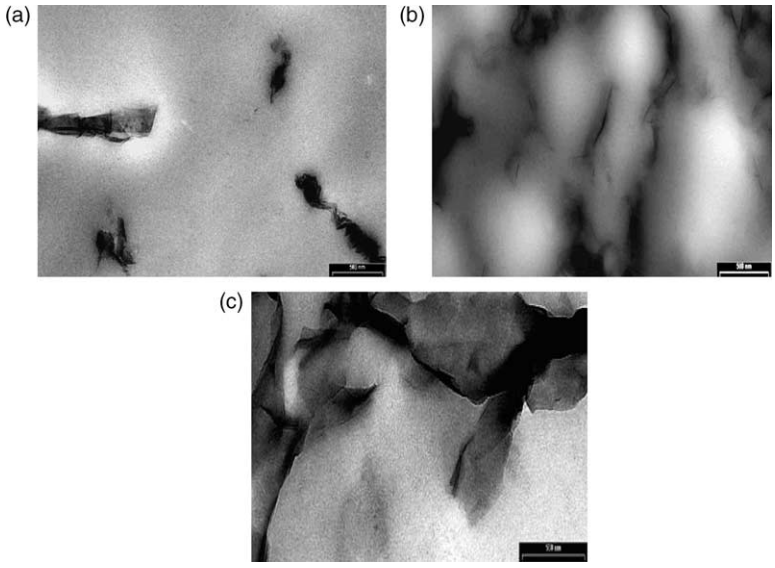

Fig. 2. Transmission electron micrographs of (a) commercial clay; (b) sodium bentonite and (c) sodium fluorohectorite filled latex nanocomposites (7.5 phr).

The impact of nano and conventional micro fillers on the free volume and gas barrier properties of styrene butadiene rubber (SBR) has been carried out by Wang et al. [47,48]. They also concluded that the gas permeability of SBR nanocomposite is less than carbon black filled SBR; it is revealed that the permeability of nanocomposite is mainly influenced by fractional free volume and tortuous diffusion path effects attributed to the clay platelet morphology. Free volume values obtained for nano and microcomposites are given in Table 1. The decrease in free volume values of layered silicates reinforced latex nanocomposites indicate that the positronium atoms are formed and annihilate only in the pre-existing holes of virgin polymers.

3.4. Permeation of gases through nano and micro filled latex membranes

The gas transport properties of micro and nano fillers reinforced latex membranes have been analyzed using oxygen and nitrogen gases. Nitrogen and oxygen gas permeability coefficient of filled NR, XSBR and 70:30 NR/XSBR latex membranes are shown in Fig. 3(a)–(e). It is found that the transport of gases through layered silicates filled latex membranes is lower than conventional micro filled samples. The enhancement in gas barrier properties of nano clay reinforced latex membranes indicate strong polymer/filler interaction resulting in more tortuous path for the permeant molecules to travel through the membranes. Since the chain segments get immobilized in the presence of layered silicates, the free volume decreases and as a result the gas permeability coefficient reduces. Utracki and co-workers [49] studied the reduced free volume available in the polymer matrix after the incorporation of clay platelets. According to them in exfoliated polymer nanocomposite the accessible clay surface area is proportional to organo clay loading. They observed that the addition of 4 wt% of organo clay (Cloisite 15) can reduce the matrix hole fraction is twice as large as that observed for polymer nanocomposite with 2 wt% organo clay. The incorporation of 1.1 and 2.42 wt% of montmorrillonite (MMT) can reduce the matrix free volume to 4.7 and 8.0%, respectively. Upon the addition of nano clay sometimes small change can be observed due to the intercalation of the polymer into the clay layers. The schematic representation of increase in tortuosity upon the addition of fillers is shown in Fig. 4. Tortuosity factor is the ratio of the actual distance that a penetrant must travel to the shortest distance that it would travel in the absence of layered silicates.

Table 1
PALS measurements data of layered silicates and micro fillers reinforced (2.5 phr) NR, XSBR and 70:30 NR/XSBR latex membranes

Sample	Relative fractional free volume	*o*-Ps life time, τ_3 (ns)	*o*-Ps intensity, I_3 (%)
N_{100sP}	23.8	2.27	19.2
$N_{100sP}E$	21.4	2.21	18.1
$N_{100sP}F$	12.8	2.14	11.5
$N_{100sP}C$	24.6	2.25	20.1
$N_{100sP}Si$	24.6	2.27	19.8
N_{0sP}	13.6	1.85	16.1
$N_{0sP}E$	12.3	1.82	15.1
$N_{0sP}F$	12.1	1.82	14.9
$N_{0sP}C$	18.1	1.84	16.8
$N_{0sP}Si$	21.6	2.11	17.5
N_{70sP}	19.7	2.10	18.3
$N_{70sP}E$	18.6	2.13	16.8
$N_{70sP}F$	17.7	2.15	15.9
$N_{70sP}C$	20.5	2.19	18.7
$N_{70sP}Si$	21.6	2.13	18.6

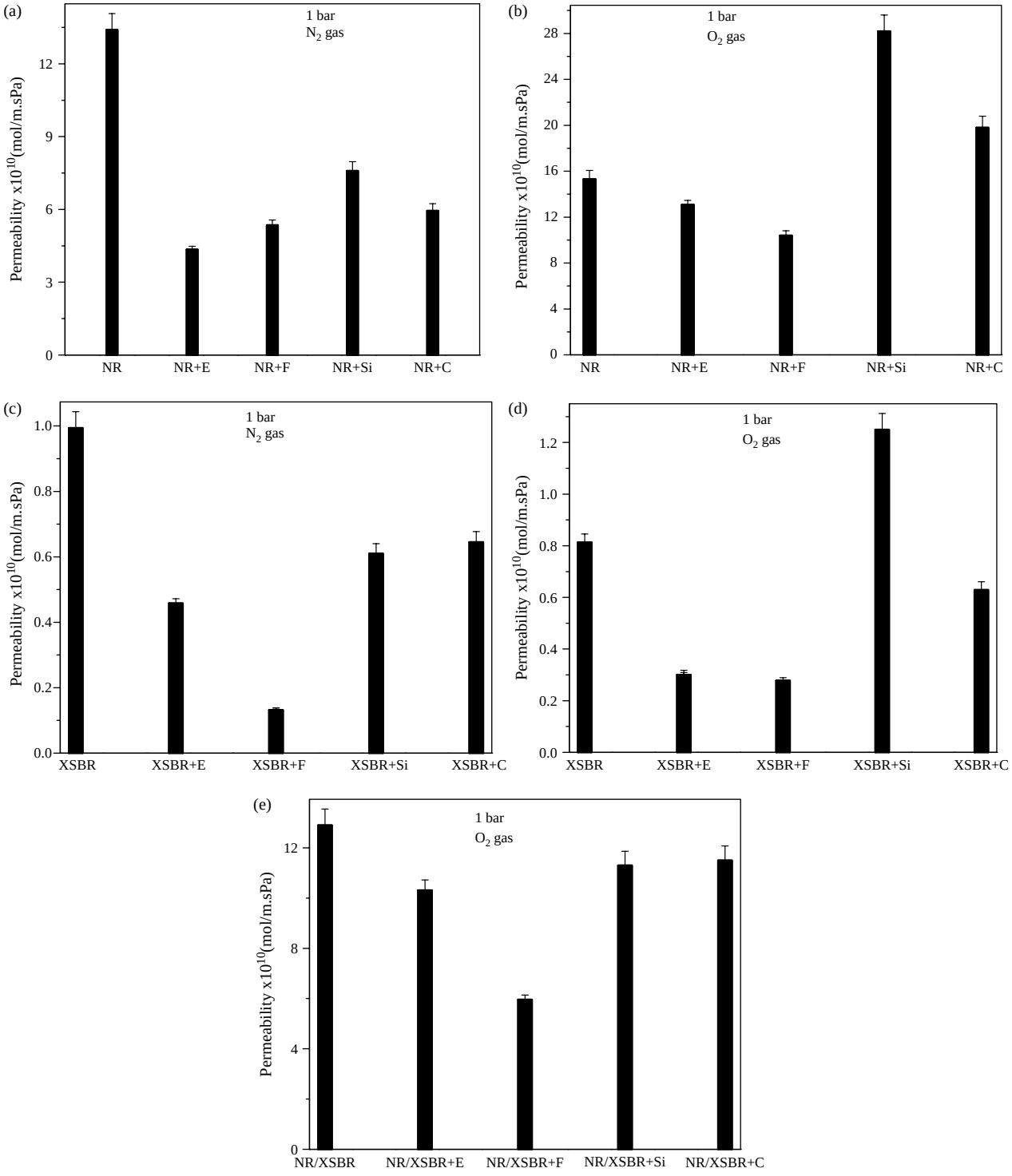

Fig. 3. (a) Variation in permeability of nitrogen gas through NR latex membrane towards different fillers (2.5 phr) at 1 bar. (b) Variation in permeability of oxygen gas through NR latex membrane towards different fillers (2.5 phr) at 1 bar. (c) Variation in permeability of nitrogen gas through XSBR latex membrane towards different fillers (2.5 phr) at 1 bar. (d) Variation in permeability of oxygen gas through XSBR latex membrane towards different fillers (2.5 phr) at 1 bar. (e) Variation in permeability of oxygen gas through 70:30 NR/XSBR latex membrane towards different fillers (2.5 phr) at 1 bar.

4. Discussions

4.1. Characterization of latex nanocomposites

X-ray diffraction method has been used to characterize the formation and structure of polymer–silicate hybrids by monitoring the position, shape and intensity of the basal reflection from the silicate layers. When insertion of polymer chains in the silicate layers occurs, an increase of silicate interlayer volume and corresponding layer spacing could be obtained which intact give rise to the shifting of diffraction peaks to lower angles. Diffraction peak cannot be seen in the

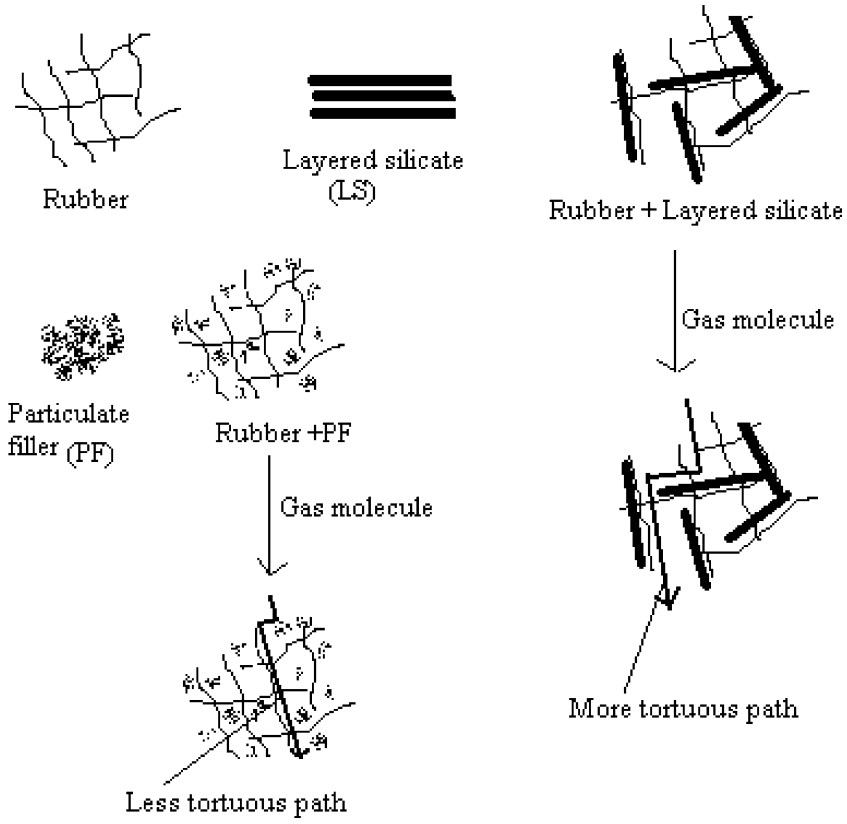

Fig. 4. Schematic representation of tortuous path formed on the addition of layered silicates and micro fillers to latex for gas transport.

case of exfoliated structures where silicate layers are completely and uniformly dispersed in a continuous polymer matrix. Fig. 1 shows the X-ray diffractograms of layered silicates and latex nanocomposites. Sodium bentonite clay exhibits a single peak at an angle 2θ of 7° corresponding to a basal spacing of 1.24 nm. The synthetic silicate sodium fluorohectorite has two peaks at 2θ of 8 and 9.5° corresponding to a basal spacing of 1.15 and 0.94 nm, respectively. As shown in Fig. 1, the basal spacing of Na-bentonite filled NR is shifted to 1.33 and 0.92 nm, indicating that the NR chains get entered into the galleries of Na-bentonite. Na-fluorohectorite filled NR show a broad peak at a basal spacing of 1.28 nm. Sodium bentonite and fluorohectorite filled XSBR shows peaks at a d spacing of 1.46 and 0.93 and 1.46 and 1.29 nm, respectively. The basal spacing of XSBR latex nanocomposite is higher than NR and is attributed to the polarity of XSBR latex. As a consequence, the polymer matrix gets partially exfoliated into the silicate layers. Lack of polar groups in NR may impede further delamination of silicate and form intercalated nanocomposite. From these results, it can be concluded that the intercalation of rubber chains into the silicate galleries can occur during latex stage mixing. With the help of mechanical shear the aqueous phase in the rubber latex is capable to separate the stacks into individual layers. From Fig. 1, it is found that in all systems the interlayer spacing increases due to the intercalation of polymer into the layers of layered silicates. Enhanced interlayer distance indicates that the layered structure is retained because of the formation of intercalated nanocomposite.

4.2. Morphology of latex nanocomposites

The dark lines in the transmission electron micrographs show dispersion of silicates in rubber matrix. It can be seen that the commercial clay exists as large aggregates and is unable to undergo exfoliation (Fig. 2(a)). Fig. 2(b) and (c) are the TEM pictures of sodium bentonite and fluorohectorite filled natural rubber latex nanocomposites. On comparing the dispersion of two silicates in latex, fluorohectorite exhibits more exfoliated structure than bentonite clay. In the latter case we can see partially exfoliated and intercalated structure. Most of the dispersed units of bentonite filled nanocomposites are not individual layers but layer of bundles. The silicates having the ability to swell in the aqueous phase of the latex resulting in the separation of layers. The aqueous swell ability is higher for fluorohectorite and therefore it exhibits more exfoliated structure.

4.3. Free volume measurements

The diffusion of permeant through polymeric membranes can be described by two theories, viz., molecular and free volume theories. According to free volume theory the diffusion is not a thermally activated process as in molecular model but it is assumed to result from random redistributions of free volume voids within a polymer matrix. Cohen and Turnbull [50,51] developed the free volume models that describe diffusion process when a molecule moves into void larger than a critical size; V_c. Voids are formed during the statistical redistribution

of free volume within the polymer. Polymer free volume is represented as V_f and is defined as $V_f = V - V_s$, where V is the specific volume and V_s is the specific molecular volume due to steric size and thermal vibrations. The theory of Cohen–Turnbull is given by,

$$D = D_0 \exp\left[\frac{\gamma V_c}{V_f}\right] \tag{3}$$

where γ is an overlap factor ($\gamma \approx 1$, for most polymers). This theory is not applicable for polymers far below T_g and at high temperature because the chain motions are arrested below T_g but at higher temperature an activation energy term is needed. Fujita [52] relates the thermodynamic diffusion coefficient, D_T and fractional free volume of the polymer, V_f by,

$$D_T = RTA_d \exp\left[-\frac{B_d}{V_f}\right] \tag{4}$$

where A_d is related to the size and shape of the permeant by,

$$A_d = \frac{\sigma^2}{M^{1/2}} \tag{5}$$

where M is the molecular weight of the permeant, σ is the Lennard–Jones size parameter and B_d is a parameter describing the amount of free volume needed. Fujita's theory is based on the assumption that a diffusing molecule can only move from one place to another when the local free volume around that molecule exceeds a certain critical value.

The effect of layered silicates such as sodium bentonite and fluorohectorite and the conventional micro fillers on *o*-Ps life time (τ_3), *o*-Ps intensity (I_3(%)) and relative fractional free volume which are presented in Table 1. It is found that the relative fractional free volume of virgin polymers decreases upon the addition of layered silicates. The decrease is attributed to the interaction between layered silicates and polymer due to the platelet structure and high aspect ratio of layered silicates. But the effect of micro fillers on free volume is rather complex. It shows increased relative fractional free volume values, which may be due to the aggregation of fillers and the consequent additional void formation. Layered silicates filled NR and XSBR have reduced *o*-Ps lifetime because the Ps atoms formed can annihilate only through the free volume holes present in the virgin polymer. The decrease is explained to the restricted mobility of the chain segments in the presence of layered silicates. In the case of blend system, due to the uneven distribution of silicates it shows enhanced Ps lifetime. The intensity of Ps decreases with the addition of layered silicates and is attributed to the restricted mobility of chain segments resulting in reduced free volume concentration or relative fractional free volume. The contact surface area between the filler and the matrix is higher in nanocomposites owing to its high aspect ratio, which in turn reduce the free volume concentration. However, micro filled systems exhibit increase in the intensity (I_3) of *o*-Ps indicating the poor interfacial wetting ability due to the aggregation of fillers leading to the formation of micro cavities at the interface.

4.4. Permeation of gases through filled latex membranes

In most of the cases microcomposites exhibit increase in gas permeation due to the aggregation of particles resulting in the formation of voids, Fig. 3(a)–(e). As described earlier the increase in permeation of microcomposites is explained to the presence of micro cavities at the interfacial region. The increase in gas barrier properties of latex membranes reinforced with layered silicates are due to the exfoliation of silicates in the polymer matrix leading to the nanometric level dispersion of the organic and inorganic phases. The presence of aqueous phase in latex can easily disperse the silicate particles into individual layers. The molecular level of polymer/filler interaction results in reduced availability of free volume and as a result the permeability of latex membranes decreases. The poor gas barrier properties of micro filled systems as compared to those with layered silicates is attributed to the poor physical and chemical interaction between the organic and inorganic components leading to the aggregation of fillers. The enhanced gas barrier property of nano filled latex membranes are owing to its platelet like morphology and high aspect ratio of fillers. Due to the high aspect ratio of layered silicates the contact surface area between the filler and the matrix increases. The tortuosity of the diffusion path of gas molecules in the presence of layered silicate is shown in Fig. 4. The activation energy needed for the diffusion of trapped molecules from one cavity to another one is related to cohesive energy density by the equation developed by Meares [53] and is given by,

$$E_D = \frac{\pi}{4\sigma^2 \lambda N_A (\mathrm{CED})} \tag{6}$$

where σ^2 is the cross section of the penetrant molecule, λ is the jump length and N_A is Avogadro's constant. Due to the polarity of XSBR latex its cohesive energy density is high and hence the permeability of gases through these membranes is very less. The addition of fillers further enhances its gas barrier properties.

The effect of penetrant size on the diffusion of gas molecules through these membranes can also be understood from the Fig. 3(a)–(e). As compared to nitrogen, oxygen has more permeability than nitrogen due to the lower covalent radii of oxygen. This can be explained by using Stoke–Einstein equation; according to them the diffusion of gas molecules is inversely related to the friction exerted. The equation is given by,

$$D = \frac{k_B T}{f} \tag{7}$$

Where k_B is the Boltzmann constant, T is the absolute temperature and f is the friction factor. As the radius of the gas molecule increases the friction factor also increases by the relation,

$$F = 6\pi\mu R_0 \tag{8}$$

and thereby the permeability decreases. Where μ is the viscosity of the solvent and R_0 is the radius of the diffusing gas molecule.

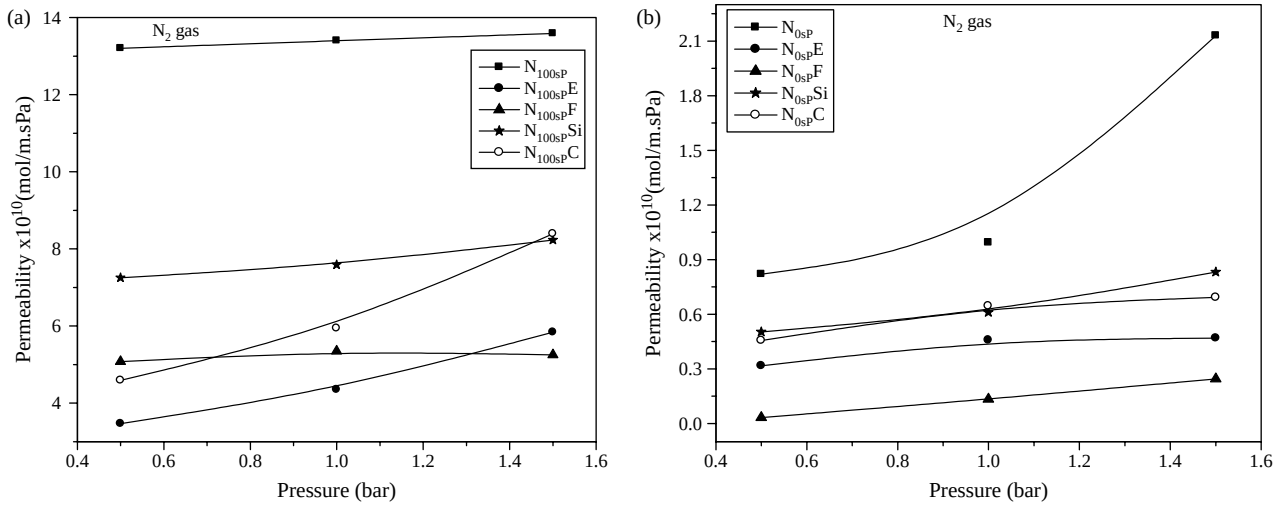

Fig. 5. (a) Effect of pressure on the permeability of nitrogen gas through filled (2.5 phr) NR latex membrane. (b) Effect of pressure on the permeability of nitrogen gas through filled (2.5 phr) XSBR latex membrane.

The permeation mechanism can be elucidated by examining the variation in permeability coefficient as a function of pressure [54]. The effect of pressure on the nitrogen gas permeability of NR latex with nano and micro fillers are given in Fig. 5(a). Sodium bentonite and micro filled systems show marginal effect of pressure on the gas transport properties. While rest of the systems are almost independent of the pressure exerted due to the close packing of fillers in the polymeric materials, especially for fluorohectorite filled system. A plot of variation in permeability with pressure of nano and microcomposites of XSBR membrane is given in Fig. 5(b). The unfilled XSBR system exhibits increase in permeability with pressure. This is due to the higher solubility of permeant molecule in the polymer chain as a function of pressure. The permeability of filled XSBR system increases slightly with pressure. From the results we can conclude that the effect of pressure on the permeability of all systems is negligible.

The addition of fillers reduces gas permeability of polymers according to a tortuous path model, developed by Neilson [55],

$$P_c = P_p\left[\frac{1-\phi_f}{1+\alpha\phi_f/2}\right] \quad (9)$$

where P_c and P_p are the permeability of composite and polymer, ϕ_f is the volume fraction of filler and α is the aspect ratio of platelets.

Schematic representation of the tortuous path model is given in Fig. 6. From this it is clear that the gas molecules have to travel through a tortuous path in the presence of layered silicate. The effect of filler loading on the permeation of gases through nano and microcomposites of NR is shown in Fig. 7(a). The gas permeability of silicates filled polymer system decreases constantly with filler loading due to the tortuous path the gas molecule has to travel in the presence of layered silicates. The reduced gas permeability of nanocomposites is influenced by two factors, viz, geometry of the filler and the molecular level interaction of the matrix and the filler. Due to the platelet like morphology of silicates, the nano filled matrix exhibit reduced permeability owing to the increase in tortuosity of path. Due to the high aspect ratio, the nano fillers exhibit more exfoliated structure. As seen in TEM pictures the extent of exfoliation is higher for fluorohectorite. Therefore, fluorohectorite filled system exhibit reduced gas permeability due to high polymer/filler interaction resulting in reduced free volume. The influence of aspect ratio on the permeability of gases can be determined from Nielsen equation (Eq. (9)). As the aspect ratio of filler increases the permeability coefficient decreases due to the enhancement in tortuosity of the path. In contrast, the gas permeability of microcomposites increases as a function of filler loading. This can be explained in terms of aggregation of fillers with increase in concentration of filler resulting in the weakening of polymer chain. Due to the low aspect ratio of filler the microcomposites show non-exfoliated aggregated structure because of the poor polymer/filler interaction. This will result in the formation of micro cavities at the interfacial region. The high gum strength of NR latex and the lack of active centers will enhance the aggregation of conventional filler. The structural peculiarity of layered silicates is the reason for the enhancement in gas barrier

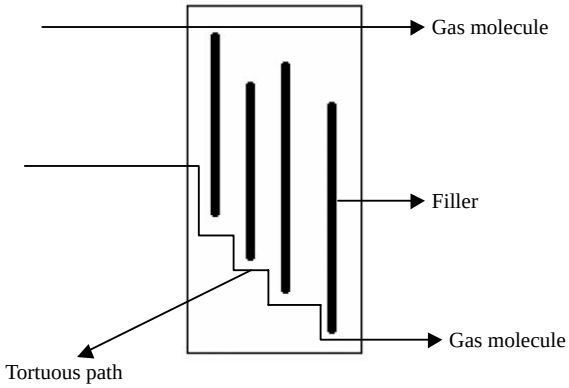

Fig. 6. Schematic representation of the tortuous path model developed by Nielsen for the transport of gases through filled membranes.

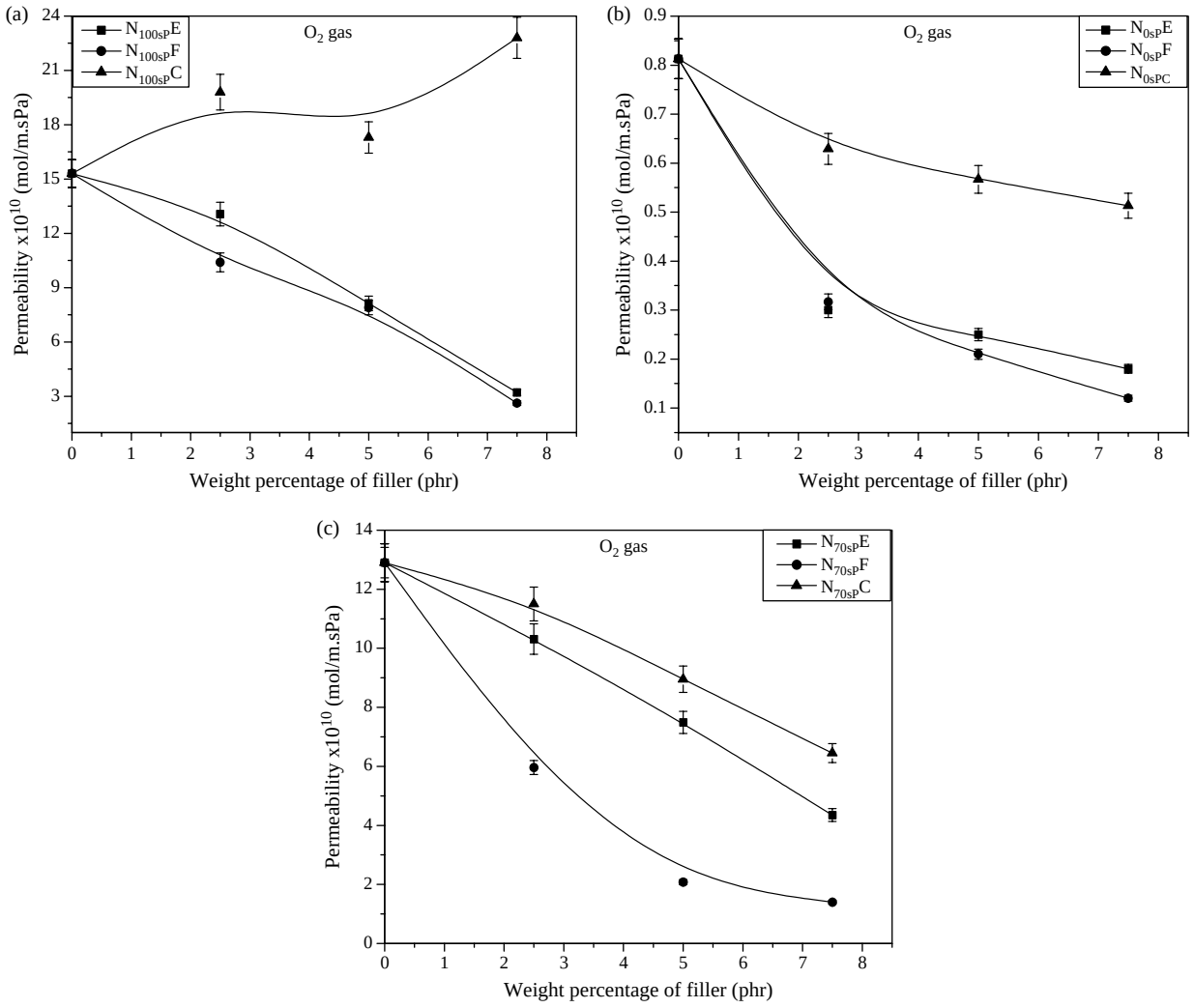

Fig. 7. (a) Effect of filler loading on the permeability of oxygen gas through NR latex membrane at 1 bar. (b) Effect of filler loading on the permeability of oxygen gas through XSBR latex membrane at 1 bar. (c) Effect of filler loading on the permeability of oxygen gas through 70:30 NR/XSBR latex membrane at 1 bar.

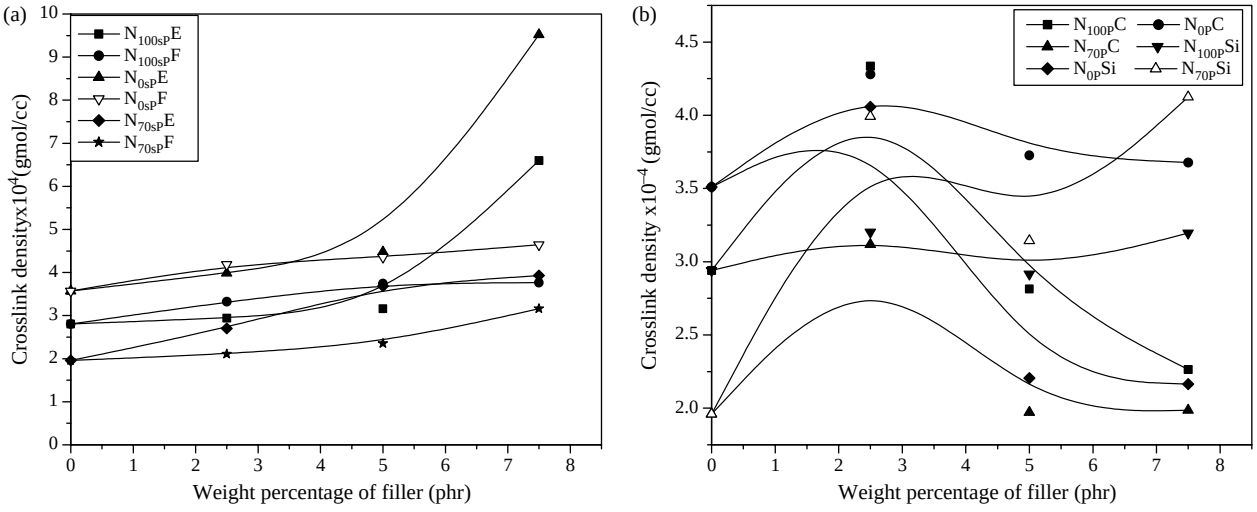

Fig. 8. (a) Crosslink density variation of layered silicates reinforced NR, XSBR and 70:30 NR/XSBR latex membranes. (b) Crosslink density variation of micro fillers reinforced NR, XSBR and 70:30 NR/XSBR latex membranes.

properties of NR latex membrane with the addition of filler. The aqueous medium of NR latex can easily disperse the platelets of silicates into individual layers. Fig. 7(b) and (c) are the plots of variation in gas permeability of nano and microcomposites of XSBR and 70:30 NR/XSBR latex membranes as a function of filler concentration. It is interesting to note that in these two systems the gas barrier properties enhanced with the increment in the weight percentage of filler. The decrease in gas permeability is sharp for nano systems owing to its higher polymer/filler interaction. Gas permeability coefficient of micro filled XSBR and 70:30 NR/XSBR decreases as a function of filler loading but the change is not as sharp as seen in layered silicates reinforced systems.

4.5. Crosslink density measurements

The crosslink density values give a clear picture about the matrix/filler interaction. The crosslink density (ν) can be calculated from swelling method using the equation,

$$\nu = \frac{1}{2M_c} \tag{10}$$

M_c is the molecular weight of polymer between crosslinks.

$$M_c = \frac{-\rho_r V_s V_{rf}^{1/3}}{\ln[1-V_{rf}] + V_{rf} + \chi V_{rf}^2} \tag{11}$$

ρ_r is the density of polymer,V_s is the molecular weight of solvent and χ is the interaction parameter, V_{rf} is the volume fraction of rubber in the solvent-swollen filled sample. V_{rf} is given by the equation of Ellis and Welding [56],

$$V_{rf} = \frac{(d-fw)/\rho_P}{d-fw/\rho_P + A_s/\rho_s} \tag{12}$$

where d is the deswollen weight, f is the volume fraction of the filler, w is the initial weight of the sample,ρ_p is the density of the polymer, ρ_s is the density of the solvent, and A_s is the amount of solvent absorbed

For an unfilled system $f=0$.

The interaction parameter, χ is given by Hildebrand equation [57,58],

$$\chi = \beta + \frac{V_s(\delta_s-\delta_p)^2}{RT} \tag{13}$$

β is the lattice constant, V_s is the molar volume, R is the universal gas constant, T is the absolute temperature, δ_s is the solubility parameter of solvent and δ_p is the solubility parameter of polymer.

Fig. 8(a) is the plot of crosslink density values of NR, XSBR and 70:30 NR/XSBR filled with layered silicates. In most of the cases, the crosslink density increases with filler loading. In the present case, the amount of solvent absorbed by the sample (A_s) decreases and hence the V_{rf} value increases leading to higher crosslink density. The increase in crosslink density of polymers with layered silicates signifies the reinforcement of clay in the polymer and as a result the stiffness of the material increases. The variation in crosslink density with filler loading for micro filled latex systems is shown Fig. 8(b). At 2.5 phr of filler all the systems exhibit sharp increase in crosslink density. Higher crosslink density values mean more restraint on the network and thus results in lower swelling due to the presence of fillers. However, at higher concentration of filler the crosslink density is found to decrease due to the absorption of curatives on the surface of filler particles. The decrease in crosslink density observed in microcomposites due to the aggregation of filler is also a reason for the enhancement in gas permeability.

4.6. Estimation of degree of reinforcement

The reinforcement of layered silicates in latex systems can be analyzed from Kraus plot [59]. The Kraus equation is given by,

$$\frac{V_{ro}}{V_{rf}} = 1 - m\left(\frac{f}{1-f}\right) \tag{14}$$

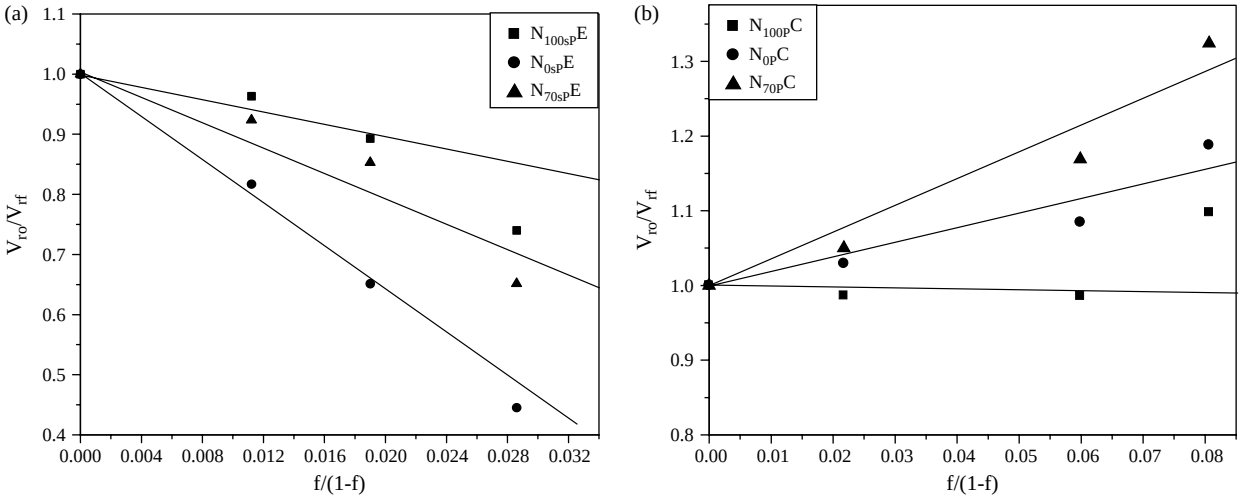

Fig. 9. (a) Kraus plot of sodium bentonite filled NR, XSBR and 70:30 NR/XSBR latex membranes. (b) Kraus plot of micro filled (clay) reinforced NR, XSBR and 70:30 NR/XSBR latex membranes.

A plot of V_{ro}/V_{rf} against $f/(1-f)$ shows the extent of reinforcement caused by fillers in various polymeric materials. In equation (14), V_{ro} is the volume fraction of rubber phase in swollen gel of gum rubber vulcanizate and is given by,

$$V_{ro} = \frac{d/\rho_P}{(d/\rho_P) + (A_s/\rho_S)} \quad (15)$$

V_{ro} is constant for a particular system.

V_{rf} is the volume fraction of rubber phase in swollen gel of filled rubber vulcanizate and is calculated using Eq. (12). f is the volume fraction of filler in the rubber vulcanizate, m is the slope of the Kraus plot and the value of it gives the degree of interaction of polymer and filler.

The Kraus plot of Na-bentonite filled NR, XSBR and 70:30 NR/XSBR are presented in Fig. 9(a). According to this theory the negative slope (m) value is an indication of reinforcement of filler in the matrix. The higher the negative slope, the greater the degree of reinforcement. Layered silicates reinforced systems exhibit negative slope values due to the higher reinforcing capability of layered silicates occurred by the intercalation of polymer into the layers of silicates. The solvent uptake of the sample decreases in the presence of layered silicates, which is associated with the tortuous path. This will result in enhancement of V_{rf} value consequently the value of V_{ro}/V_{rf} ratio decreases, because V_{ro} is constant. From the slope values, it can be concluded that the degree of reinforcement increases in the order $N_{0sP}E > N_{70sP}E > N_{100sP}E > N_{osP}C > N_{100sP}C > N_{70sP}C$. A plot of V_{ro}/V_{rf} against $f/(1-f)$ of micro filled NR, XSBR and 70:30 NR/XSBR are given in Fig. 9(b). It can be seen that the Kraus plots deviate from the horizontal line in different degrees to upward direction, give positive m value for NR and 70:30 NR/XSBR, indicating poor rubber/filler interaction. The m value of clay filled XSBR is negative. This is explained to the high polymer/filler interaction due to the polarity of XSBR latex. It can easily exchange the cations with the layered silicates. The slope (m) values are presented in Table 2.

4.7. Selectivity of membranes

The polymeric membranes used for gas separation processes have certain significance such as high permeability to the desired gas, high selectivity and the ability to form useful membrane configurations. The requirement of an ideal membrane is high permeability together with high permselectivity. The permselectivity of a membrane is given by,

Table 2
The slope m values obtained from Kraus plot for layered silicates and micro fillers reinforced NR, XSBR and 70:30 NR/XSBR latex membranes

Sample	Kraus equation slope (m)
$N_{100sP}E$	−8.96
$N_{0sP}E$	−19.48
$N_{70sP}E$	−11.84
$N_{100sP}C$	0.98
$N_{0sP}C$	2.17
$N_{70sP}C$	3.85

Table 3
Oxygen-to-nitrogen selectivity values of unfilled and filled (2.5 phr) sulphur prevulcanized NR, XSBR and 70:30 NR/XSBR latex membranes

Sample	Permselectivity ($P(O_2)/P(N_2)$)
N_{100sP}	1.14
$N_{100sP}E$	3.00
$N_{100sP}F$	1.94
$N_{100sP}C$	3.33
$N_{100sP}Si$	3.71
N_{0sP}	1.02
$N_{0sP}E$	1.52
$N_{0sP}F$	2.40
$N_{0sP}C$	1.03
$N_{0sP}Si$	1.93
N_{70sP}	1.89
$N_{70sP}E$	2.47
$N_{70sP}F$	3.29
$N_{70sP}C$	2.29
$N_{70sP}Si$	1.48

$$\alpha(O_2, N_2) = \frac{P(O_2)}{P(N_2)} \quad (16)$$

where α is the permselectivity of a membrane towards O_2 and N_2 gas, $P(O_2)$ and $P(N_2)$ are the permeability constants of O_2 and N_2 gases, respectively.

The permselectivity values of filled NR, XSBR and 70:30 NR/XSBR latex membranes are given in Table 3. The nanocomposites possesses higher selectivity than the micro-composites. These might be ascribed to the interaction between the polymer and the filler. The introduction of silicates into NR latex has varied effects on the selectivity of membranes. Compared to nitrogen gas the NR latex membrane containing micro fillers is highly permeable to oxygen gas and thereby the selectivity of these membranes increases.

The selectivity and permeability of these membranes can be further understood from the diffusivity and solubility values. The permeability of a polymeric material is the product of diffusivity and solubility. It is usually represented as,

$$P = DS \quad (17)$$

where P is the permeability coefficient, D is the diffusivity and S is the solubility. The diffusivity D is a kinetic parameter related to the size of the permeant and to the polymer-segment mobility. The solubility factor S is a thermodynamic parameter, which depends on the polymer/permeant interaction [6]. The diffusion coefficient, D is calculated by the time-lag method using the equation,

$$D = \frac{x^2}{6t'} \quad (18)$$

where x is the thickness of the sample and t' is the time-lag, i.e. the time needed to attain the steady-state condition. Table 4 tabulates the N_2 and O_2 gas diffusivity and diffusive selectivity values of filled and unfilled NR, XSBR and 70:30 NR/XSBR latex membrane. The diffusion coefficient of E filled NR is lower than other filled systems. It can be seen that the diffusivity values of nano filled NR is lower than other systems. This is due to the reduction in the overall segmental mobility in

Table 4
Diffusion coefficient and selectivity values of NR, XSBR and 70:30 NR/XSBR latex membranes with layered silicates and micro fillers (2.5 phr) for oxygen and nitrogen gas

Sample	$D\times10^8$ cm^2/s		$D(O_2)/D(N_2)$
	O_2 gas	N_2 gas	
N_{100sP}	3.2	2.93	1.09
$N_{100sP}E$	0.05	0.05	1.00
$N_{100sP}F$	0.83	0.63	1.32
$N_{100sP}C$	3.25	2.71	1.19
$N_{100sP}Si$	3.12	2.95	1.15
$N_{0s}P$	2.87	2.46	1.17
$N_{0sP}E$	0.34	0.28	1.21
$N_{0sP}F$	0.47	0.28	1.68
$N_{0sP}C$	1.81	1.5	1.21
$N_{0sP}Si$	1.96	1.68	1.17
$N_{70s}P$	3.2	2.95	1.08
$N_{70sP}E$	0.58	0.39	1.49
$N_{70sP}F$	0.56	0.39	1.44
$N_{70sP}C$	3.85	3.43	1.12
$N_{70sP}Si$	3.13	3.43	1.25

the presence of inorganic fillers, particularly at the interfacial phase surrounding the silica particles. The fluorohectorite filled system shows higher diffusion selectivity values. The gas diffusion coefficient of nano filled membranes exhibit lower values than the conventionally filled and unfilled systems. It is interesting to note that the diffusion selectivity of nano filled latex membranes is higher than other systems. These membranes show a drastic decrease in diffusion coefficient values, it is ascribed to the comparatively homogeneous distribution of nano particles in the polymer chain resulting in the compact packing between the polymer chains and the nanoparticles. It is also well known that the crosslinking indeed causes a decrease in the total amount of free volume in the polymer chain. Sulphur prevulcanized latex membranes are used for these experiments. Crosslinked polymeric systems show a remarkable reduction in diffusivity. The crosslinking and the presence of layered silicates decreases the segmental mobility and hence the diffusion process.

5. Conclusions

The gas transport properties of nano and micro filled NR, XSBR and 70:30 NR/XSBR blend latex membranes were investigated using permanent gases such as O_2 and N_2. Due to the enhanced polymer/filler interaction, the nanocomposites exhibited lower permeability to oxygen and nitrogen gases. The higher reinforcement of layered silicates in latex membrane is associated with its platelet like morphology and high aspect ratio. The free volume in the latex membranes decreased in the presence of layered silicates and can be explained in terms of the confinement of the chain segments. Micro filled samples showed higher permeability and this is ascribed to the poor physical interaction between the polymer and filler leading to aggregation of fillers. The size of the penetrant gas molecule affected the permeability coefficient. The covalent radii of nitrogen gas molecule are higher than oxygen gas molecule and hence nitrogen gas showed reduced permeability.

From the plots of pressure against permeability, we can understand that there was not much effect of pressure on the permeability of gas molecules through these latex membranes. As the filler loading increased the permeability of polymer containing layered silicate decreased due to the increase in tortuosity of path. However, the reverse effect could be seen in samples with conventional micron sized fillers. This was explained in terms of the aggregation of filler particles. The crosslink density of the filled samples was computed by equilibrium swelling method. The crosslink density values were found to be higher for layered silicates reinforced latex membranes supporting polymer/filler interaction. The degree of reinforcement was determined from Kraus plot; the negative slope value for nano filled samples indicated the high degree reinforcement of nano fillers in the rubber matrix. However, micro filled systems gave positive slope values, which indicated poor rubber/filler interaction. Compared to NR, synthetic latex and its blend showed higher selectivity than micro and unfilled systems. Micron sized fillers incorporated polymeric membranes exhibited higher diffusion coefficient. Finally it is important to mention that by the incorporation of nano fillers into rubbers; new gas barrier membranes could be developed.

Acknowledgements

One of the authors Ms Ranimol Stephen is thankful to Council of Scientific and Industrial Research (CSIR), New Delhi for providing the Senior Research Fellowship.

References

[1] Koros WJ, Mahajan R. J Membr Sci 2000;175:181.
[2] Koros WJ, Fleming GK. J Membr Sci 1993;83:80.
[3] Scott K, Hughs R. Industrial membrane separation technology. Bishopbriggs: Chapman and Hall; 1996.
[4] Cornelius CJ, Marand E. J Membr Sci 2002;202:97.
[5] Moon EJ, Yoo JE, Choi HW, Kim CK. J Membr Sci 2002;204:283.
[6] Naylor T. Permeation properties in handbook of comprehensive polymer science, vol. 2, 1 and 643 edn, UK: Pergamon Press; 1989.
[7] Compan V, Zanuy D, Andrio A, Morillo M, Aleman C, Guerra SM. Macromolecules 2002;35:4521.
[8] Arnold ME, Nagai K, Freeman BD, Spontak RJ, Betts DE, De Simone JM, et al. Macromolecules 2001;34:5611.
[9] Barbi V, Funari SS, Gehrke R, Scharnagl N, Stribeck N. Macromolecules 2003;36:749.
[10] Pixton MR, Paul DR. Macromolecules 1995;28:8277.
[11] Vega MA, Paul DR. J Polym Sci, Polym Phys Ed 1993;31:1577.
[12] Aitken CL, Koros WJ, Paul DR. Macromolecules 1992;25:3651.
[13] Mc Hattie JS, Koros WJ, Paul DR. Polymer 1992;33:1701.
[14] Mc Hattie JS, Koros WJ, Paul DR. Polymer 1991;32:2618.
[15] Tiemblo P, Guzman J, Riande E, Mijangos C, Reinecke H. Macromolecules 2002;35:420.
[16] Neilson PW, Xu GF. Macromolecules 1996;29:3457.
[17] Aithal US, Balundgi RH, Aminabhavi TM, Shukla SS. Polym-Plast Technol Eng 1991;30(4):299.
[18] van Amerongen GJ. J Appl Phys 1946;17:972. van Amerongen GJ. Rubber Chem Technol 1947;20:494.

[19] van Amerongen GJ. J Polym Sci 1950;5:307. van Amerongen GJ. Rubber Chem Technol 1951;24:10.
[20] Johnson T, Thomas S. Polymer 1999;40:3223.
[21] George SC, Ninan KN, Thomas S. Eur Polym J 2001;37:183.
[22] Wang Y, Wang J. J Polym Eng Sci 1999;39:190.
[23] Wu D, Wang X, Song Y, Jin R. J Appl Polym Sci 2004;92:2714.
[24] Lopez-Manchado MA, Biagiotti J, Valentini L, Kenny JM. J Appl Polym Sci 2004;92:3394.
[25] Cho JW, Paul DR. Polymer 2001;42:1083.
[26] Fu X, Qutubuddin S. Polymer 2001;42:807.
[27] Kim GM, Lee DH, Hoffmann B, Stoppelmann G. Polymer 2000;41: 1095.
[28] Zanetti M, Lomakin S, Camino G. Macromol Mater Eng 2000;279:1.
[29] Giannelis EP. Adv Mater 1996;8:29.
[30] Kojima Y, Usuki A, Kawasumi M, Okada A, Fukushima Y, Kurauchi T, et al. J Mater Res 1993;8:1185.
[31] Hasegawa N, Okamoto H, Kato M, Usuki A, Sato N. Polymer 2003;44: 2933.
[32] Wang MS, Pinnavaia TJ. J Chem Mater 1994;6:468.
[33] Weiner MW, Chen H, Giannelis EP, Sogah DY. J Am Chem Soc 1999; 122:1615.
[34] Matayabas Jr JC, Turner SR. Nanocomposite technology for enhancing the gas barrier of polyethylene terephthalate. In: Pinnavaia TJ, Beall GW, editors. Polymer–clay nanocomposites, vol. 207. New York: Wiley; 2000 [chapter 11].
[35] Varghese S, Karger-Kocsis J. Polymer 2003;44:4921.
[36] Varghese S, Gatos KG, Apostolov AA, Karger-Kocsis J. J Appl Polym Sci 2004;92:543.
[37] Varghese S, Karger-Kocsis J, Gatos KG. Polymer 2003;44:3977.
[38] Stephen R, Thomas S, Joseph K. J Appl Polym Sci 2005;98:1125.
[39] Stephen R, Raju KVSN, Nair SV, Oommen Z, Thomas S. J Appl Polym Sci 2003;88:2640.
[40] Ravikumar HB, Ranganathaiah C, Kumaraswamy GN, Thomas S. Polymer 2005;46:2372.
[41] Nakanishi H, Jean YC. In: Schrader DM, Jean YC, editors. Positron and positronium chemistry. Amsterdam: Elsevier; 1988. p. 159.
[42] Jean YC. Microchem J 1990;42:72.
[43] Tanaka K, Kawai T, Kita H, Okamoto K, Ito Y. Macromolecules 2000;33: 5513.
[44] Kobayashi Y, Haraya K, Hattori S, Sasuga T. Polymer 1994;35:925.
[45] Ito K, Saito Y, Yamamoto T, Ujihira Y, Nomura K. Macromolecules 2001;6153:18.
[46] Nagel C, Gunther-Schade K, Fritsch D, Strunskus T, Faupel F. Macromolecules 2002;35:2071.
[47] Wang ZF, Wang B, Qi N, Zhang HF, Zhang LQ. Polymer 2005;46:719.
[48] Wang YQ, Wu YP, Zhang HF, Zhang LQ, Wang B, Wang ZF. Macromol Rapid Commun 2004;25:19773.
[49] Utracki LA, Simha R. Macromolecules 2004;37:10123.
[50] Turnbull D, Cohen MH. J Chem Phys 1961;34:120.
[51] Cohen MH, Turnbull D. J Chem Phys 1959;31(5):1164.
[52] Fujita H, Kishimoto AJ. J Polym Sci 1958;28:547.
[53] Meares P. In: Crank J, Park GS, editors. Diffusion in polymers. New York: Academic Press; 1968.
[54] Mizoguchi K, Terada K, Naito Y, Kamiya Y, Tsuchida S, Yano S. Colloid Polym Sci 1997;86:275.
[55] Neilson LE. J Macromol Sci (Chem) 1967;A1(5):929.
[56] Ellis B, Welding GN. Techniques of polymer science. London: Society for Chemical Industry; 1964. p. 46.
[57] Hildebrand JH, Scott RL. The solubility of non-electrolyte. 3rd ed. New York: Van Nostrand Reinhold; 1950.
[58] Hildebrand JH, Scott RL. Regular solutions. Englewood Cliffs, NJ: Prentice-Hall; 1962.
[59] Kraus G. J Appl Polym Sci 1963;7:861.